Fizika Nizkikh Temperatur, 2005, v. 31, No. 5, p. 585–589

Hysteretic phenomena in Xe-doped C_{60} from x-ray diffraction

A.I. Prokhvatilov[1], N.N. Galtsov[1], I.V. Legchenkova[1], M. A. Strzhemechny[1], D. Cassidy[2], G.E. Gadd[2], S. Moricca[2], B. Sundqvist[3], and N.A. Aksenova[4]

[1]*B. Verkin Institute for Low Temperature Physics and Engineering of the National Academy of Sciences of Ukraine, 47 Lenin Ave., Kharkov 61103, Ukraine*
E-mail: galtsov@ilt.kharkov.ua

[2]*Australian Nuclear Science and Technology Organisation, Private Mail Bag 1, Menai, NSW 2234, Australia*
E-mail: geg@ansto.gov.au

[3]*Department of Physics, Umea University, S-901 87 Umea, Sweden*

[4]*Rail Way Transport Academy, 23 Moskovski Ave., Kharkov, Ukraine*

Received August 4, 2004, revised August 10, 2004

Polycrystalline fullerite C_{60} intercalated with Xe atoms at 575 K and a pressure of 200 MPa was studied by powder x-ray diffraction. The integrated intensities of a few brighter reflections have been utilized to evaluate the occupancy of the octahedral interstitial sites in C_{60} crystals, which turned out to be (34±4) %, and in good agreement with another independent estimate. It is found that reflections of the (h00) type become observable in Xe-doped C_{60}. The presence of xenon in the octahedral sites affects both the orientational phase transition as well as the glassification process, decreasing both characteristic temperatures as well as smearing the phase transition over a greater temperature range. Considerable hysteretic phenomena have been observed close to the phase transition and the glassification temperature. The signs of the two hysteresis loops are opposite. There is reliable evidence that at lowest temperatures studied the thermal expansion of the doped crystal is negative under cool-down.

PACS: 61.10.Nz, 81.05.Tp, **64.70.−p**

Introduction

The cubic crystals of fullerite C_{60} comprise almost spherical molecules with a diameter of 10.2 Å. The lattice has quite large interstitial cavities with octahedral (4.12 Å) and tetrahedral (2.2 Å) point symmetry, which can be stuffed with various atoms or molecules with sizes comparable to the void diameters. This circumstance was utilized at the very beginning of the fullerene era resulting in the high-T_c superconductivity of an organic crystal (C_{60} doped with alkali metals) [1]. Afterwards, C_{60} was intercalated with rare gas atoms [2–7] and molecules of different symmetries and sizes [8–14]. It is commonly accepted that changes in the physical properties of fullerite C_{60} brought about by intercalation with neutral species are mainly due to the doping-related change in the molar volume. In the particular case under study the doped crystal can be considered either to be under a negative pressure or, in the opposite sense, to exhibit a positive internal pressure.

The most interesting phenomena caused by intercalation are observed within the regions where the orientational phase transition (T_c = 260 K) occurs or the orientational glass forms (T_g = 90 K). Usually, when the voids are filled with the larger rare gas atoms such as Xe or with simpler closed-shell molecules, the anisotropic interaction between C_{60} molecules weakens; and the rotation of the C_{60} molecules loosens up, resulting in lower critical temperatures for both transformations [6,7]. Moreover, when the dopant species are certain molecules, for example, CO or NO, there are indications [15,16] that no freezing into an orientational

glass state was observed. In regards to doping with rare gas species, both large negative expansivity as well as temperature hysteresis of the thermal expansion are observed at low temperatures [17].

In this paper, we report detailed powder x-ray studies of the structural characteristics of Xe-doped C_{60}, with a temperature cycling around the orientational phase transition (150–300 K) as well as in the region where orientational glass states tend to form, (7 to 100 K).

Experimental

C_{60} powder was saturated with xenon at a pressure and temperature of about 200 MPa and 575 °C, respectively, for a period of 36 hours. When intercalated at high pressure but at 300 °C, only 10% of octahedral voids are filled; the filling can reach 66% if C_{60} is saturated at 575 °C [6]. In the present case, thermogravimetric analysis (TGA) showed a weight loss between 6 and 7% indicative of a stoichiometry of $Xe_{0.39–0.45}C_{60}$. The powder of Xe-doped C_{60} was subsequently compacted for dilatometric studies in cylindrical dies by quasi-hydrostatic compression with pressures of up to 1 GPa, as described elsewhere [17]. The sample used in our x-ray experiments was a chunk taken from the larger compacted specimen, the smooth surface of which served as the reflection plane in the x-ray experiments.

Powder x-ray studies were carried out on a DRON-3M diffractometer equipped with a special liquid-helium cryostat. The temperature of samples was varied over the range of 7 to 300 K. The temperature was stabilized to within ±0.05 K at every measurement point. In the orientational glass domain ($T < 70$ K) and below the orientational phase transition point ($T_c = 260$ K), the temperature was varied in warm-up and cool-down regimes with the intention of looking for possible hysteretic phenomena of the lattice parameters and thermal expansivities. The intensities, widths, and angular positions of the relevant reflections as functions of temperature were used for analysis of the phenomena under study. The lattice parameter error was ±0.02 % and the intensity of the x-ray reflections was measured to within 1 %.

Results and discussion

A typical x-ray pattern is shown in Fig. 1. It can be seen that our fine-grain samples, in addition to the fcc phase of Xe-doped fullerite C_{60}, contain about 10% of another phase which could in no way be indexed as fcc. It should be noted that in the «as-prepared» Xe-doped powder samples, no other than but fcc phase was detected [6] either in x-ray or neutron diffraction experiments. The reflections belonging to this new

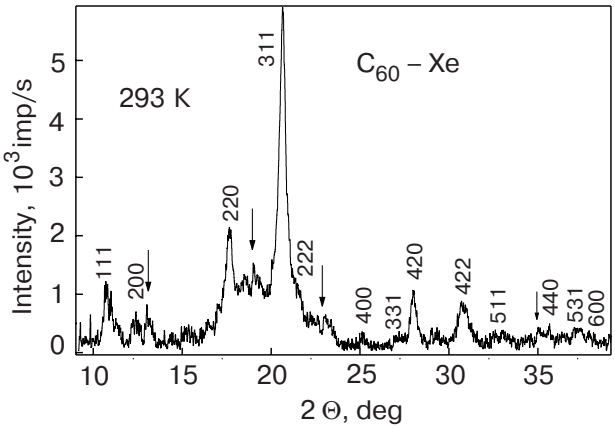

Fig. 1. A typical x-ray diffraction pattern from polycrystalline C_{60}–Xe samples, recorded at room temperature. The indexed reflections belong to the orientationally disordered fcc phase of Xe-doped fullerite C_{60}. The arrows indicate reflections of an unknown phase.

phase are indicated in Fig. 1 with arrows. It is possible that the new phase is a result of a partial polymerization caused by the previous compacting. Notwithstanding the known polymerization-related structure [18,19] we failed to find a space group that could fit the extra reflections mentioned.

We observed substantial changes in the scattered intensities compared to pure fullerite. To mention first, the reflections of the type (h00) became clearly distinguishable (in pure C_{60} their intensities are virtually zero because of the specific molecule / lattice size relation and the shape of C_{60} molecule [20]). Some other reflections, such as (111) and (220), are lower in intensities as compared to pure C_{60}, while others such as (420) and (422), are brighter.

The absolute lattice parameter values as a function of temperature were determined as follows. At two reference points, viz., at room temperature and at 7 K, full-profile diffraction patterns have been recorded in order to obtain the rms averaged reference cubic lattice parameter values for those two reference points and in each case with the lattice parameter averaged over all the observed reflections. Then, between those two reference points, the lattice parameters at other temperatures was determined from the (311) reflection and scaled appropriately to the reference values.

Using these lattice parameters, we calculated how the intercalation with Xe has changed the room-temperature diffraction intensity ratios for specifically chosen reflections compared to the most intense (311) reflection, as a function of the occupancy of octahedral voids by Xe atoms and assuming a uniform distribution of the dopant throughout the sample. In the calculations we used the following expression for the scattering amplitude of reflection (hkl):

$$F(q) \propto 60 f_C(\mathbf{q})(\sin qr/qr + f_{RG}(\mathbf{q}) X_{RG}(-1)^{h+k+l}. \quad (1)$$

Equation (1) generally applies for the case of atoms of any rare gas randomly distributed over octahedral cavities. The first term in the right-hand side of Eq. (1) is the contribution from the randomly rotating C_{60} molecules; the second term is the contribution from the interstitial rare gas (RG) atoms. The quantities $f_C(\mathbf{q})$ and $f_{RG}(\mathbf{q})$, both functions of the momentum transfer vector, are respectively the carbon and RG atomic scattering factors and $f_{Xe}(\mathbf{q})$ will be used for the latter. The absolute magnitude of the vector $\mathbf{q}$ is given by $4\pi\sin(\theta)/\lambda$, where 2θ is the deflection angle of the incident x-rays with wavelength λ. Finally, X_{RG} is the rare gas occupancy of the octahedral voids, which is assumed to be uniform throughout the sample. The square of $F(\mathbf{q})$ in Eq.(1) is proportional to the intensity of the actual x-ray reflections at the respective angles 2θ, the values were calculated using the lattice parameter determined as described from the room-temperature value $a = (14.246\pm0.003)$ Å. Integrated intensities were determined using the Gaussian function which turned out to be a little better than the Lorentzian one. All calculated integrated intensities were normalized to that of the brightest reflection (311). The experimentally determined integrated intensity ratios for the chosen reflections are plotted in Fig. 2 to evaluate the occupancy of octahedral voids by xenon. Using the four occupancies thus found (see Fig. 2), we calculated the weighted average of the occupancy to be $X_{Xe} = (34\pm4)\%$, in good agreement with previously found TGA data $(41.5 \pm 2.5)\%$, see above in the Experimental Section). We ascribe the uncertainty in the value to two factors, viz., the inhomogeneity of the distribution of Xe over the grain volume and the errors in absolute intensity values for the weaker lines (see Fig. 2).

Variations of the lattice parameter $a(T)$ of Xe-doped C_{60} with temperature under warm-up and cool-down are plotted in Fig. 3. One can see that the path $a(T)$ depends essentially on the direction of temperature variation. Two hysteresis loops were observed and it is noteworthy that the signs of the warmup/cooldown hystereses are opposite to each other. At temperatures below the orientational phase transition in pure fullerite ($T_c = 260$ K), the cool-down lattice parameters are appreciably higher than those found with warm-up. In the temperature range where the orientational glass is observed in pure C_{60} the hysteresis loop has a narrower span and, as mentioned above, its sign is opposite to that of the hysteresis at higher temperatures, or in other words, the cool-down lattice parameter values are smaller than the warmup ones.

Repeated cooldown of the sample virtually did not change the situation and the lattice parameter $a(T)$ followed the same path as found during the first cool-down run. What is striking is the strong «smearing» and shift of the orientational transition to lower temperatures, as compared to that for pure C_{60}, as well as the huge temperature span of the hysteresis loop, which stretches from 150 K up to room temperature. The largest lattice parameter difference at 230 K amounts to $\Delta a = 0.055$ Å, which exceeds by far the experiment error in $a(T)$. The hysteretic effect observed at lower temperatures affects the crystal lattice to a lesser extent. The loop is found to be far from symmetric; the upper bifurcation point is at $T = (60\pm5)$ K; whilst the maximum lattice parameter difference $\Delta a = (0.007\pm0.003)$ Å is reached at ~ 20 K. A pronounced instability was observed for the cool-down regime, which manifested itself in a greater scatter of lattice parameter values. The cool-down curve is steeper than the warm-up curve at the high-temperature end of

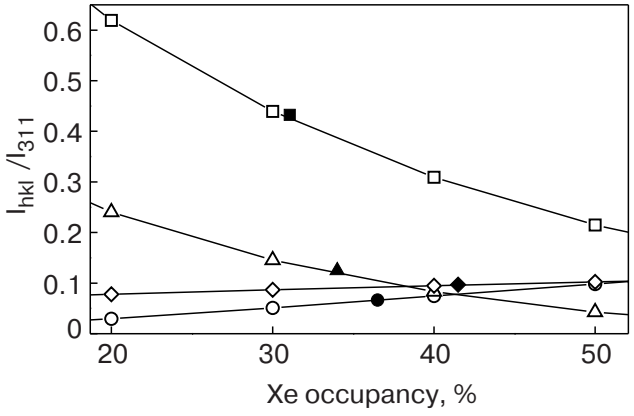

Fig. 2. Calculated intensity ratios for a few fcc reflections versus the Xe occupancy of octahedral voids at room temperature with the lattice parameter equal to a = 14.246 Å: 220 (□), 222 (△), 420 (◇), 200 (○). The solid symbols indicate the corresponding experimental intensity ratios.

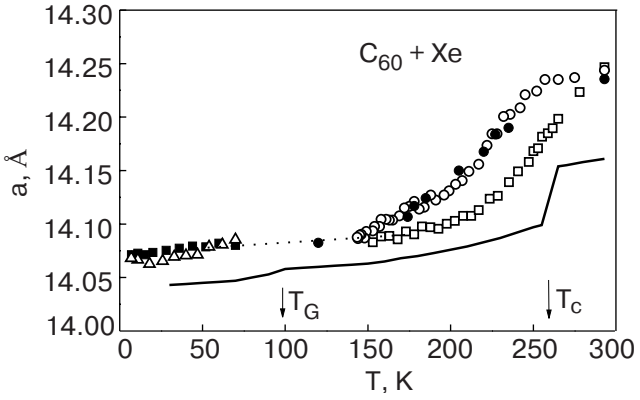

Fig. 3. Temperature dependence of the lattice parameter of the C_{60}–Xe sample, as measured under cool-down or warm-up regimes: warm-up (□), (■); cool-down (○), (●), (△); pure C_{60} (–). The lower solid curve is for pure fullerite C_{60} [22].

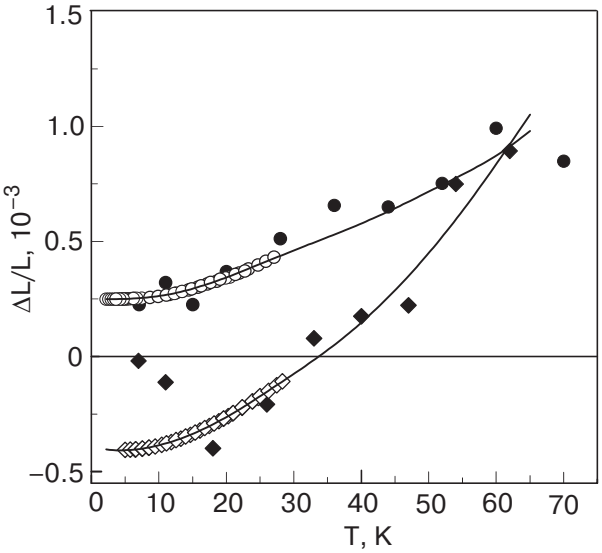

Fig. 4. Relative elongation versus temperature polycrystalline C_{60}–Xe samples under warm-up and cool-down, according to dilatometric [24] and x-ray diffraction measurements; cool-down: this work (◆), [24] (◇); warm-up: this work (●), [24] (○)..

the hysteresis loop. What is equally striking is that at the low-temperature end there is a definite indication that the thermal expansivity has become negative. A very rough estimate from the three lowest points yields unusually large negative expansivities of the order of $-5{\cdot}10^{-4}$ K^{-1}. Negative linear thermal expansion coefficients at low temperatures have already been documented for pure fullerite [21] and also for fullerite intercalated with neon, argon, and krypton [17,23] and now, in conjunction with this work, with Xe as well [23]. The dilatometric measurements of thermal expansion coefficients in the orientational glass region of the C_{60}–Xe system have been carried out up to 28 K. Which allowed comparison between dilatometric of Ref. 24 and x-ray data, as shown in Fig. 4. The solid curves are drawn through dilatometry points and smoothly extrapolated to higher temperatures. A good qualitative agreement is evident.

We tried to observe relaxation processes in the domain of the high-temperature hysteresis at fixed temperatures of 150, 180, 220 and 250 K on both the warm-up and cool-down branches. Contrary to our expectations, no changes in lattice parameter values were recorded and this was even after quite long (10 hours) waiting times.

The cause behind the anomalies observed in this report (two hystereses, large negative expansivities at low temperatures) is not completely clear. A qualitative explanation of both low-temperature anomalies (the hysteresis and the negative expansivities) was suggested by Aleksandrovskii et al. [24]. The negative expansion coefficients, found dilatometrically at low temperatures [24], are related to the tunnel nature of the low-energy levels. The hysteresis is ascribed to a polyamorphic phase transition between two different orientational glass phases, in which case the non-ergodic character of the glass system can lead to hysteretic phenomena. As regards the high-temperatures hysteresis, we can make the following remarks. Of course, since the orientational phase transition is a first-order one, it is quite natural that it occurs with a hysteresis. We understand but well that because the distribution of Xe atoms inside the crystallites should be, most likely, highly inhomogeneous, the span of the hysteresis could be much larger than in pure C_{60} [22]. However, first, the temperature span is too broad and, second, the high-temperature bifurcation point is (contrary to expectations) above T_c in the pure material. So, the nature of the high-temperature hysteresis is not completely understood.

Considering the lattice parameter of C_{60} doped with Xe as a function of the occupancy X_{Xe} (see Fig. 5) we note that the specific occupancy as estimated from our x-ray diffraction data (Fig.2) falls close to the points from other reports [6] that dealt with the C_{60}–Xe system. However, if taken in their completeness the points of the $a(X_{Xe})$ dependence do not fall on a straight line. For other rare gas species as dopants of C_{60}, and where the lattice parameter vs. occupancy is known it appears to follow a linear $a(X_{RG})$ relationships. This is clearly seen in Fig. 5 for Ne [25]. Indirect evidence from our findings on the C_{60}–He system [26,27], also suggests is a linear function, whereas for Ar the span of X_{Ar} is too narrow to make a sound judgment at this stage. The

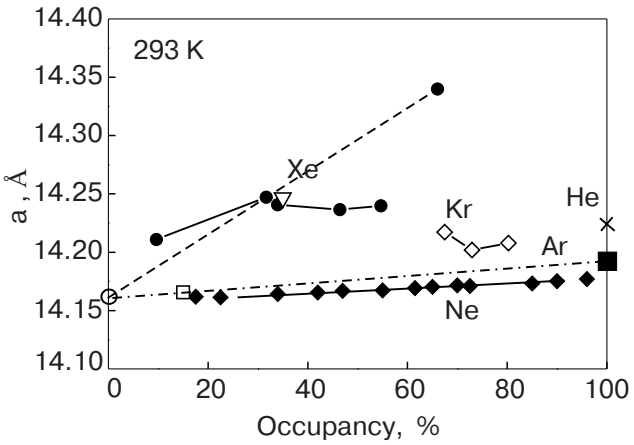

Fig. 5. The lattice parameter of RG-doped cubic fullerite C_{60} as a function of the RG occupancy of octahedral voids. The corresponding references are: the solid circles [6] and the empty overturned triangle is from this study for Xe; the solid rhombs [3] for Ne; the empty rhombs [6] for Kr; the solid [5,6] and empty (this work, see text) squares for Ar; the tilted cross [26,27] for He; the open circle for pure C_{60} [22].

reason behind the nonlinearity of the $a(X_{Xe})$ relationship is not clear at present.

Conclusions

We have performed x-ray powder diffraction studies of a Xe-doped C_{60} sample over the temperature range from 7 to 300 K.

The sample is found to contain two phases. One is the fcc phase, quite common for fullerite C_{60} but with the lattice parameter slightly increased due to xenon present. The structure of the other phase (of approximately 10% content) was not determined. Its presence might result from partial polymerization brought about by sample preparation handling.

The room temperature reflection intensities allowed us to evaluate the weight averaged Xe occupancy as (34±4) mol %, in good agreement with the TGA estimates performed upon saturation.

The variation of the fcc lattice parameter with temperature depends strongly on the sign of the temperature increment. Two hysteresis loops have been observed in the temperature dependence of the lattice parameter. The wider and more pronounced one is below the orientational transition point; the other hysteresis loop is below the orientational glassification point ($Tg < 70$ K). The nature of the hysteresis, especially of the high-temperature one, is not completely clear.

The lattice parameters measured in the lowest temperature points under cooldown give indication of unusually large negative thermal expansivities.

The authors thank A.N. Aleksandrovskii and V.G. Manzhelii for valuable discussions and for providing us with their experimental results prior to publication. This work was partially supported by the STCU, Grant No 2669.

1. O. Zhou and D.E. Cox, *J. Phys. Chem. Solids* **11**, 1373 (1992).
2. J.E. Schirber, G.H. Kwei, J.D. Jorgensen, R.L. Hitterman, and B. Morosin, *Phys. Rev.* **B51**, 12014 (1995).
3. B. Morosin, J.D. Jorgensen, S. Short, G.H. Kwei, and J.E. Schirber, *Phys. Rev.* **B53**, 1675 (1996).
4. G.E. Gadd, P.J. Evans, S. Moricca, and M. James, *J. Mat. Res.* **12**, 1 (1997)
5. G.E. Gadd, S.J. Kennedy, S. Moricca, C.J. Howard, M.M. Elcombe, P.J. Evans, and M. James, *Phys. Rev.* **B55**, 14794 (1997).
6. G.E. Gadd, S. Moricca, S.J. Kennedy, M.M. Elcombe, J. Evans, M. Blackford, D. Cassidy, C.J. Howard, P. Prasad, J.V. Hanna, A. Burchwood, and D. Levy, *J. Phys. Chem. Solids* **58**, 1823 (1997).
7. M. Gu and T.B. Tang, *J. Appl. Phys.* **93**, 2486 (2003).
8. J.E. Schirber, R.A. Assink, G.A. Samara, B. Morosin, and D. Loy, *Phys. Rev.* **B51**, 15552 (1995).
9. S.A. Meyers, R.A. Assink, J.E. Schirber, and D. Loy, *Mat. Res. Soc. Symp. Proc.* **359**, 505 (1995).
10. B. Morosin, R.A. Assink, R.G. Dunn, T.M. Massis, and J.E. Schirber, *Phys. Rev.* **B56**, 13611 (1997).
11. M. James, S.J. Kennedy, M.M. Elcombe, and G.E. Gadd, *Phys. Rev.* **B58**, 14780 (1998).
12. G.H. Kwei, F. Troun, B. Morosin, and H.F. King, *J. Chem. Phys.* **113**, 320 (2000).
13. S.A. FitzGerald, T. Yildirim, L.J. Santodonato, D.A. Neuman, J.R.D. Copley, J.J. Rush, and F. Trouw, *Phys. Rev.* **B60**, 6439 (1999).
14. I. Holleman, G. von Helden, A. van der Avoird, and G. Meijer, *Phys. Rev. Lett.* **80**, 4899 (1998).
15. S. Van Smaalen, R. Dinnebier, I. Holleman, G. von Helden, and G. Meijer, *Phys. Rev.* **B57**, 6321 (1998).
16. M. Gu, T.B. Tang, and D. Feng, *Phys. Rev.* **B66**, 073404 (2002).
17. A.N. Aleksandrovskii, A.S. Bakai, A.V. Dolbin, G.E. Gadd, V.G. Gavrilko, V.G. Manzhelii, S. Moricca, B. Sundqvist, and B.G. Udovidchenko, *Fiz. Nizk. Temp.* **29**, 432 (2003) [*Low Temp. Phys.* **29**, 324 (2003)].
18. S. Amelinks, C. Van Henrich, D. van Dyck, and G. Van Tendeloo, *Phys. Status Solidi* **A131**, 589 (1992).
19. B. Sundqvist, *Adv. Phys.* **48**, 1 (1999).
20. R. Moret, P. Launois, T. Wagberg, B. Sundqvist, V. Agafonov, V.A. Davydov, and A.V. Rakhmanina, *Eur. Phys. J.* **B37**, 25 (2004).
21. A.N Aleksandrovskii, V.B. Esel'son, V.G. Manzhelii, A.V. Soldatov, B. Sundqvist, and B.G. Udovidchenko, *Fiz. Nizk Temp.* **23**, 1256 (1997) [*Low Temp. Phys.* **23**, 943 (1997)]; *Fiz. Nizk. Temp.* **26**, 100 (2000) [*Low Temp. Phys.* **26**, 75 (2000)].
22. N.A. Aksenova, A.P. Isakina, A.I. Prokhvatilov, M.A. Strzhemechny, *Fiz. Nizk. Temp.* **25**, 964 (1999) [*Low Temp. Phys.* **25**, 724 (1999)].
23. A.N. Aleksandrovskii, V.G. Gavrilko, V.B. Esel'son, V.G. Manzhelii, B.G. Udovidchenko, and V.P. Maletskiy, *Fiz. Nizk Temp.* **27**, 1401 (2001) [*Low Temp. Phys.* **27**, 1033 (2001)].
24. A.N. Aleksandrovskii, A.S. Bakai, A.V. Dolbin, V.B. Esel'son, G.E. Gadd, V.G. Gavrilko, V. G. Manzhelii, S. Moricca, and B. Sundqvist, *Fiz. Nizk. Temp.* 565 (2005).
25. B. Morosin, J.D. Jorgensen, S. Short, G.H. Kwei, and J.E. Schirber, *Phys. Rev.* **B53**, 1675 (1996).
26. I.V. Legchencova, A.I. Prokhvatilov, Yu.E. Stetsenko, M.A. Strzhemechny, K.A. Yagotintsev, A.A. Avdeenko, V.V. Eremenko, P.V. Zinoviev, V.N. Zoryansky, N.B. Silaeva, and R.S. Ruoff, *Fiz. Nizk. Temp.* **28**, 1320 (2002) [*Low Temp. Phys.* **28**, 942 (2002)].
27. Yu.E. Stetsenko, I.V. Legchenkova, K.A. Yagotintsev, A.I. Prokhvatilov, and M.A. Strzhemechny, *Fiz. Nizk. Temp.* **29**, 597 (2003) [*Low Temp. Phys.* **29**, 445 (2003)].